Multi-Channel Electronic Stethoscope for Enhanced Cardiac Auscultation using Beamforming and Equalisation Techniques

Shahab Pasha
STC Research Centre
Mid Sweden University
Sundsvall, Sweden
shahab.pasha@miun.se

Jan Lundgren
STC Research Centre
Mid Sweden University
Sundsvall, Sweden
jan.lundgren@miun.se

Christian Ritz
School of Electrical, Computer, and Telecommunication Engineering
University of Wollongong
Wollongong, Australia
critz@uow.edu.au

***Abstract*—This paper reports on the implementation of a multi-channel electronic stethoscope designed to isolate the heart sound from the interfering sounds of the lungs and blood vessels. The multi-channel stethoscope comprises four piezo contact microphones arranged in rectangular and linear arrays. Beamforming and channel equalisation techniques are applied to the multi-channel recordings made in the aortic, pulmonary, tricuspid, and mitral valve areas. The proposed channel equaliser cancels out the distorting effect of the chest and rib cage on the heart sound frequency spectrum. It is shown that the applied beamforming methods effectively suppress the interfering lung noise and improve the signal to interference and noise ratio by 16 dB. The results confirm the superior performance of the implemented multi-channel stethoscope compared with commercially available single-channel electronic stethoscopes.**

Keywords*—*Beamforming, Channel equalisation, Chest acoustics, Microphone arrays, Multi-channel electronic stethoscope

I. INTRODUCTION

Heart auscultation can be traced back to ancient civilizations such as those in Greece and Egypt, although we lack information about the tools used. The stethoscope as we know it was invented by Laënnec in 1816, and since then significant advances have been made in heart condition diagnosis by auscultation [1]. Classic stethoscopes comprising a diaphragm and a hollow air-filled tube suffer numerous drawbacks, such as low sensitivity, high background noise, frequency band distortion, and no quantitative measurement [1]. More advanced electronic stethoscopes use an electret microphone along with the diaphragm and replace the tube with a wire to overcome the noise issue [2].

Despite recent advances in electronic stethoscope design [3] and technology [4, 5], and although new stethoscopes apply basic signal processing techniques such as digital filtering and amplification [2, 6], all commercially available electronic stethoscopes are still single-channel devices. Single-channel electronic stethoscopes cannot benefit from more effective multi-channel signal processing methods such as multi-channel noise cancelation, beamforming, and source separation.

To overcome this limitation, researchers have proposed multi-sensor chest sound acquisition systems [7] for heart sound imaging [8, 9] and 3D heart sound localisation [10]. In the context of medical and biological signal processing in which the signals (e.g., heart and lung sounds) overlap in the frequency domain and are attenuated significantly by muscle and fat tissues, it is of great interest to separate and amplify the signals effectively.

This research studies chest acoustics [11] and designs and implements a multi-channel electronic stethoscope to cancel the frequency spectrum distortions (caused by the rib cage and the muscle tissues) and isolate the heart sound from the chest acoustic mix. The proposed system uses minimum variance distortionless response (MVDR) beamforming and baseline delay and sum beamforming (DSB) designed for the linear and rectangular arrays of four microelectromechanical system (MEMS) microphones. The proposed stethoscope also reduces the number of sensors required for accurately analysing the heart sound (e.g., from 36 [12]), giving a cleaner output signal than do heart sound mapping systems [12] and single-channel electronic stethoscopes.

The rest of the paper is organised as follows. A brief mathematical model of the chest acoustics and the heart and lung sounds is presented in section II. The design of the array geometries is discussed in section III. The channel equaliser and beamformers are proposed in sections IV and V, respectively. The proposed multi-channel stethoscope is compared with a single-channel stethoscope under different test conditions in section VI. The paper concludes in section VII.

II. CHEST ACOUSTICS AND THE HEART SOUND

Analysis of chest acoustics suggests that the rib cage and the muscle tissues covering the surrounding area act as a low-pass filter, attenuating frequencies above 1000 Hz as sound travels through the chest cavity [13]. Study of the biomedical signals also show that the main frequency components of the heart sound are below 500 Hz. Although the chest filters out some of the lung noise [14], heart sound recordings made on the chest surface still contain significant noise and interfering signals. Under certain circumstances (e.g., obesity), heart sound auscultation is unsuccessful if advanced separation and amplification techniques are not applied.

The signal observed by an M-sensor stethoscope (Fig. 1) is mathematically modelled as an array of

$$x_m(n) = h_m^s(n) * s(n) + h_m^l(n) * l(n) + v(n), \qquad (1)$$

where $x_m(n)$ is the mix recorded by sensor $m \in \{1, \dots, M\}$, $s(n)$ is the heart sound, $l(n)$ is the bronchial/vesicular lung sounds [1], and $\mathbf{h}_m^s$ and $\mathbf{h}_m^l$ are the acoustic response of the chest at sensor m location to the heart valves and lungs,

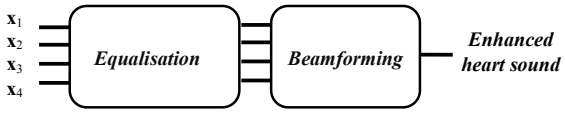

Fig. 1: Proposed multi-channel stethoscope

respectively; $v(n)$ represents the noise from the examination area and rustling. As the target heart sound is a narrow-band signal ranging from 20 to 500 Hz, the recorded mix ($\mathbf{x}_m$) is usually filtered by a low-pass filter with a 500-Hz threshold and 80 dB/octave attenuation to remove the high-frequency interference ($l(n)$) and noise ($v(n)$) (1).

Collecting the observations from the M sensor array, $\mathbf{X} = \{\mathbf{x_1}, \dots \mathbf{x}_M\}$ (Fig. 1), the goal is to extract $s(n)$ from $\mathbf{X}$.

A. Chest acoustic transfer function

In this study, the frequency response of the human chest is limited to the heart sound frequency band. The transfer function of the chest, $\mathbf{h}_m^s$ (1), is modelled as

$$\mathbf{h}_m^s = \frac{A_n(f,\varphi)}{\|r_s - r_m\|} \times e^{-\frac{j2\pi\|r_s - r_m\|}{c}}, \qquad (2)$$

where $\|r_s - r_m\|$ is the distance between the target valve location, r_s, and the sensor location, r_m, c is the speed of sound in the body [15, 16] (TABLE **1**), and $A_n(f,\varphi)$ represents the chest's acoustic response at different frequencies and angles of arrival. The acoustic transfer function of the chest wall attenuates the higher frequencies by 80 dB/octave [14].

A chirp signal with a time period of $T = 5\,sec$ and a frequency range of 0–500 Hz, providing a flat power spectrum, is used to obtain the human body's frequency response. The signal is played through a loudspeaker at the back of a dummy (at the left mid scapular line) and the response is recorded at the top of the aorta by a stethoscope (Fig. *2*).

B. Interference from lungs and the cardiovascular system

The human chest acts as a complex sound source, including the heart, respiratory system, and cardiovascular system. The chest (including the rib cage and muscle and fat tissues) also attenuates, filters, and distorts the frequency spectrum of the generated sound (2) [14]. Notably, the speed of sound differs between tissues, for example, being higher in bones (2117 m s⁻) than in the lungs (949 m s^{-1}) [15].

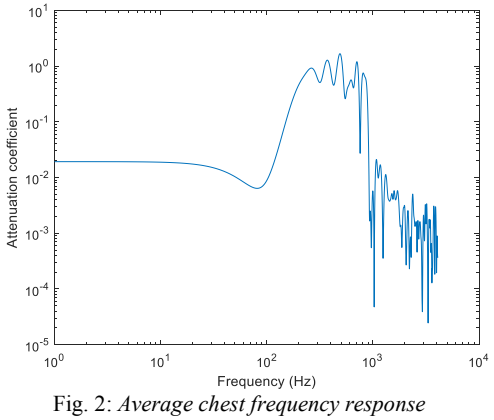

Fig. 2: *Average chest frequency response*

TABLE 1: SIGNAL AND ARRAY PROPERTIES

Average speed of sound in chest	1540 m s^{-1} [15, 16]
Operating wavelength (λ)	2.9 m (290 cm)
Average chest acoustic impedance	1.5 × 10^5 rayl [11]
Largest array dimension (L)	0.08 m (8 cm)
Source to array distance (d)	Max. 10 cm
Heart sound frequency band	50–1000 Hz
Sampling frequency (f_s)	41 kHz

The lung frequency spectrum that collides with the heart frequency spectrum and comes from the area of the lung behind the heart is the noise remaining after separation and beamforming (Fig. 1).

III. Multi-channel Stethoscope Design

Studies show the average adult heart to be 11 cm × 8 cm [17] in size. Although there are small differences between males and females and different nationalities, the average dimensions are used to guide the microphone array design. In general, both main heart sounds from the tricuspid and mitral valves can be heard at all auscultation sites (Fig. *3*) [18], but some pathological and normal sounds are best heard at one site or another. The combined area of all the heart valves, which are the sound source, is considered to be around 4.5 cm^2 [17]. It is important to design a microphone array large enough to cover the area of the target valve area and small enough to capture only one sound source (i.e., valve) at a time (i.e., be dominated by only one valve's sound). A diaphragm larger than 6 cm in diameter (i.e., 115 cm^2) collects the sound from two or more adjacent valves simultaneously (Fig. *3*). Spatial aliasing is another important design criterion. The estimated distance between the targeted heart valve and the centre of the array should be 10 cm.

A. Transducer type

Electronic stethoscopes have various transducer types [19], including piezoelectric sensors, MEMS microphones, and varying-capacitance electret microphones with one fixed plate and one moveable plate on the diaphragm. It is beyond the scope of this research to investigate and compare these electronic stethoscope types [20]. However, to reduce the stethoscope size [21] to less than 9 cm^2 and fit the four channels in the area of one typical diaphragm (i.e., 50 cm^2), piezoelectric sensors [22] are chosen.

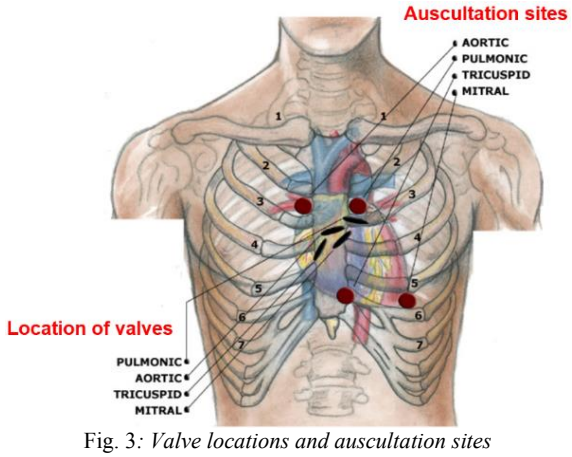

Fig. 3*: Valve locations and auscultation sites*

B. Array geometry

The goal of the array design is to arrange the sensors so as to obtain the desired response [23] in terms of directivity for the targeted narrow-band signal (i.e., the heart sound).

If the microphone array steering vector is represented by $\mathbf{z}(f,\theta)$ at frequency f and angle of arrival θ,

$$\mathbf{z}(f,\theta) = [1, \ldots, e^{-j2\pi f(J-1)}, e^{-j2\pi f\mu_1\cos\theta}, e^{-j2\pi f(\mu_1\cos\theta+1)}, \ldots, e^{-j2\pi f(\mu_1\cos\theta+(J-1))}, \ldots, e^{-j2\pi f(\mu_{M-1}\cos\theta+(J-1))}]^T, \quad (3)$$

where μ_m is the time delay between the mth channel and the reference channel and J represents the length of the tapped delay lines. The goal of the microphone array topology design is to minimise the side lobes before the beamforming. The implemented sensor arrays are a linear array of four microphones with 2-cm inter-channel spacing and a two-by-two rectangular array with 2-cm inter-channel spacing.

IV. Chest Channel Equalisaton and Amplification

The high-frequency components of heart murmurs are suppressed by the chest and surrounding muscles [14]. As the channel is time varying due to the rib cage movement and changing lung size, it is ideal to use an adaptive equaliser and to update the equaliser coefficients to track the channel changes; however, in this research a fixed filter is designed based on average chest observations. The goal is to design an equalisation filter that amplifies the first two octaves of the spectrum (0–100 Hz) by 20 dB but does not affect the third octave (100–1000 Hz). The last octave (1–10 kHz) is amplified by 30 dB (Fig. 2). As opposed to state-of-the-art electronic stethoscopes that amplify the distorted signal, here the amplification occurs after the equalisation.

Simplifying (1) to consider only the heart sound signal, $(s(n))$, as the target signal,

$$x_m(n) = h_m^s(n) * s(n) + \hat{v}(n), \quad (4)$$

where $\hat{v}(n)$ models any undesired signal, including the lung interference and background noise. The N tap equaliser is

$$\boldsymbol{r} = [r_0, r_1, \ldots, r_N]^T. \quad (5)$$

The equaliser output for an input frame of length N is

$$\mathbf{x}_m{}^T\boldsymbol{r}. \quad (6)$$

Using $s(n)$ from (1), the equalisation error signal is

$$\varepsilon = s - \mathbf{x}_m{}^T\boldsymbol{r}. \quad (7)$$

As the source signal is not always available, the inverse filter is designed to cancel out the channel effect. Assuming that the noise, $v(n)$, is negligible, (1) is rewritten in the frequency domain:

$$X(\omega) = S^p(\omega)H_n^p(\omega), \quad (8)$$

where $\omega = 2\pi f$ and $H_n^p(\omega)$ is the transfer function. The goal of the equalisation is $\min_r \mathrm{E}\{\varepsilon^2\}$:

$$\min_r E\left\{\left(s_n^p(t-\tau) - s_n^p(t-\tau) * H_n^p(n) * r_n^p(n)\right)\right\}, \quad (9)$$

where $r_n^p(n)$ is the equalisation filter for channel n and source p. The inverse function (i.e., equalisation function) is

$$R_n^p(\omega) = G^{-1}(\omega) = \frac{G^*(\omega)}{|G(\omega)|^2 + a}, \quad (10)$$

where G^* stands for the complex conjugate. Schmidt et al. [14] propose the following scheme for estimating the chest acoustic response:

$$H_{chest}(f) = \frac{|X(f)| - |S(f)|}{|P_p(f)|} - |H_{stethoscope}(f)|, \quad (11)$$

where $X(f)$ and $S(f)$ are the frequency domain representations of $x(n)$ and $s(n)$, respectively, from (1) and $P_p(f)$ is the played pink noise or the chirp signal.

V. Beamforming Methods

Beamforming is used to detect the presence of a signal, estimate the direction of arrival (DOA), and enhance a desired signal whose measurements are corrupted by noise, interference sources, and reverberation [24]. In this paper, beamformers are formulated as spatial filters that operate on the outputs of a sensor array to form a desired beam (i.e., directivity) pattern.

The far-field beamforming criterion still holds and the distance between the source (i.e., each heart valve) and stethoscope (d) exceeds $\frac{2L^2}{\lambda}$ [25], where L is the array dimension and λ the operating wavelength (TABLE 1).

A. Baseline delay and sum beamformer

The delay and sum beamformer (DSB) is a basic signal enhancement technique that time-shifts each sensor's signal by a value corresponding to the time difference of arrival (TDOA) between each sensor and the reference signal (chosen arbitrarily), averaged across the sensors (i.e., piezo sensors). DSB is a fixed beamformer targeting a certain angle of arrival applicable to scenarios in which the DOA is known. For the stethoscope, if the array is located exactly above the target valve, the angle of arrival is around zero (Fig. 4).

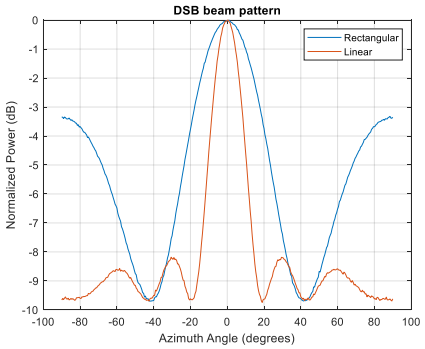

Fig. 4: DSB beam pattern

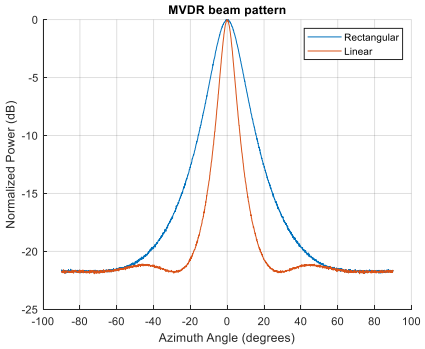

Fig. 5: *MVDR beam pattern*

$$y(n) = \frac{1}{M}\sum_{m=1}^{M} x_m(n - \tau_m). \quad (12)$$

This beamformer suppresses the ambient noise but does not significantly attenuate the lung noise interference.

$$SNR = \frac{E[(h_m^s s(n) + h_m^l l(n))^2]}{E[v(n)^2]}. \quad (13)$$

Fig. 6 illustrates the effect of beamforming on multi-channel recording. Through beamforming, the noise and interference are suppressed to levels below those of the single-channel recording.

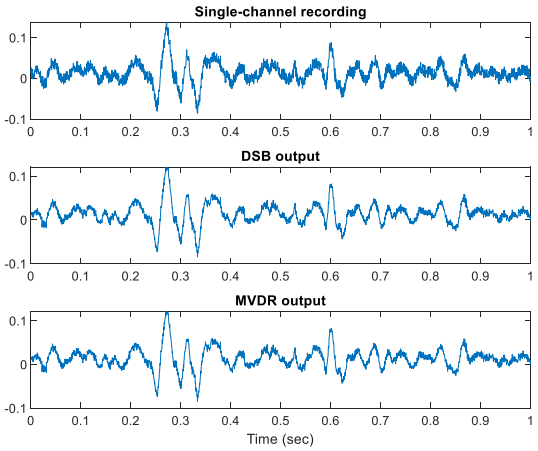

Fig. 6*: One-second heart sound beamforming results*

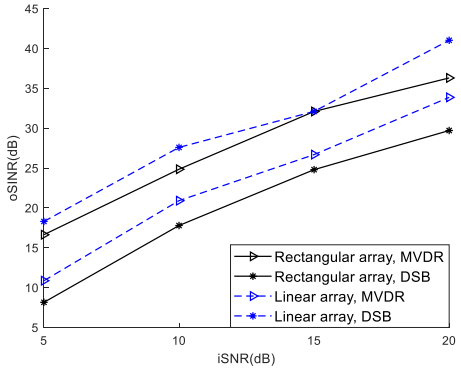

Fig. 7: *Output signal to interference and noise ratios (SINRs) for different input signal to noise ratios (SNRs)*

B. *Adaptive beamforming with MVDR*

The underlying idea is to choose the coefficients of the filter, $\mathbf{g}$, that minimise the output power, with the constraint that the desired signal, $s(n)$, is unaffected (Fig. 5-6).

$$\min_{\mathbf{g}} \mathbf{g}^T \mathbf{R}_{xx} \mathbf{g}. \quad (14)$$

where $\mathbf{R}_{xx}$ is the autocorrelation matrix of the signal. The Lagrange multiplier method can be used to solve (14):

$$\mathbf{g} = \propto_1 \frac{\mathbf{R}_{x_m x_m}^{-1} \propto}{\propto^T \mathbf{R}_{x_m x_m}^{-1} \propto}, \quad (15)$$

where $\propto$ is the attenuation factors due to propagation effects. The output of the beamformer is

$$\hat{\mathbf{x}} = \mathbf{g}^T \mathbf{x}. \quad (16)$$

VI. RESULTS AND DISCUSSION

In this section, the multi-channel stethoscope and the beamformers are tested and compared with a single-channel sensor (i.e., Thinklabs One digital stethoscope; Thinklabs, Centennial, CO, USA). The evaluation process investigates the ability of the stethoscope to suppress the lung interference at different elevation and azimuth angles.

Using (1), the signal to interference and noise ratio (SINR) is defined as

$$\text{oSINR} = \frac{|\mathbf{s}|}{|\mathbf{h}^l * \mathbf{l} + \mathbf{v}|} \quad (17)$$

The input signal includes interference and noise (1), but white noise is added to $\mathbf{x}_m$ at arbitrary levels (iSNR) (18) to allow examination of the beamformer performance at different noise levels (Fig. 7). It is concluded that DSB applied to the linear array improves the output signal quality by just under 20 dB, whereas it improves the oSINR by only 5 dB when applied to the rectangular array.

Fig. 8 represents the SINR (17) results for the DSB(12) and MVDR beamforming (15) applied to the proposed linear and rectangular arrays at different azimuth and elevation angles relative to the array origin when the stethoscope is located above the aortic valve (i.e., at the top of the sternum).

$$\text{iSNR} = \frac{\phi_{\mathbf{x}_m}}{\phi_{\mathbf{l}} + \phi_{\mathbf{v}}} \quad (18)$$

where $\phi(.)$ represents the variance of the signal.

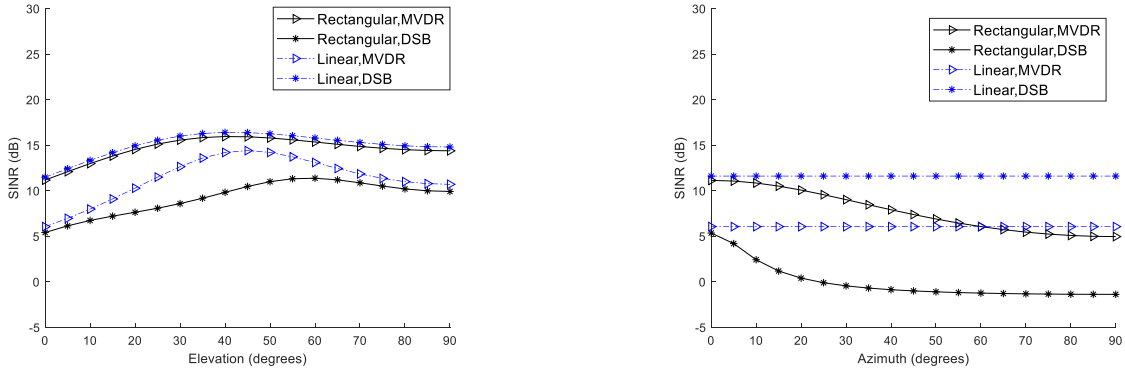

Fig. 8: *SINR results at different angles*

Although Fig. 4 and Fig. 5 show the superior performance of the MVDR beamformer compared with the DSB beamformer, the experimental studies show that that the DSB beamformer performs effectively when applied to the linear array (improving the SINR by minimum 12dB). The DSB performance is poor when applied to the rectangular array. The MVDR beamformer supresses the interference and noise more effectively when applied to the rectangular array (Fig. 8).

VII. Conclusion

A multi-channel electronic stethoscope was designed and tested for high-accuracy heart sound auscultation by removing the interfering noise. The proposed stethoscope benefits from multi-channel signal processing techniques for channel equalisation and interference suppression. It effectively targets the heart sound and suppresses the lung sound by 16 dB. This experimental study also investigated the optimal beamforming angle to achieve the cleanest heart sound when the stethoscope is located above the aortic valve. This study could be expanded on by designing and testing other microphone array geometries and transducers. Future work will focus on multi-channel source separation techniques and investigate the inter-channel spacing of the proposed stethoscope.

REFERENCES

[1] F. Dalmay, M. Antonini, P. Marquet and R. Menier, "Acoustic properties of the normal chest," *European Respiratory Journal,* no. 8, p. 1761–1769, 1995.

[2] "Stethee," [Online]. Available: https://www.stethee.com/pro.

[3] H. K. Tiwari and A. Harsola, "Development of embedded stethoscope for Heart Sound," in *International Conference on Wireless Communications, Signal Processing and Networking (WiSPNET)*, Chennai, 2016.

[4] S. Nur Hidayah Malek, W. Suhaimizan Wan Zaki, A. Joret and M. Mahadi Abdul Jamil, "Design and development of wireless stethoscope with data logging function," in *International Conference on Control System, Computing and Engineering*, Mindeb, 2013.

[5] W. Y. Shi, J. Mays and J. Chiao, "Wireless stethoscope for recording heart and lung sound," in *Topical Conference on Biomedical Wireless Technologies, Networks, and Sensing Systems (BioWireleSS)*, Austin, TX, 2016.

[6] "Thinklabs digital stethoscope," [Online]. Available: https://www.thinklabs.com/. [Accessed 10 October 2019].

[7] A. M. McKee and R. A. Goubran, "Chest sound pick-up using a multisensor array," in *SENSORS*, Irvine, CA, 2005.

[8] H. Moghaddasi, F. Almasganj and A. Zoroufian, "Imaging of heart acoustic based on the sub-space methods using a microphone array," *Computer Methods and Programs in Biomedicine,* no. 146, pp. 133-142, 2017.

[9] C. Sapsanis, "StethoVest: A simultaneous multichannel wearable system for cardiac acoustic mapping," in *Biomedical Circuits and Systems Conference (BioCAS)*, Cleveland, OH, 2018.

[10] A. Saeidi and F. Almasganj, "3D heart sound source localization via combinational subspace methods for long-term heart monitoring," *Biomedical Signal Processing and Control*, vol. 31, pp. 434–443, 2017.

[11] David A. Rice, "Transmission of lung sounds," *Seminars in Respiratory Medicine*, vol. 6, no. 3, pp. 166–170, January 1985.

[12] M. Okada, "Chest wall maps of heart sounds and murmurs," *Computers and Biomedical Research*, vol. 15, no. 3, pp. 281–294, 1981.

[13] V. Korenbaum and A. Tagil'tsev, "Acoustic properties of a human chest," *Acoustical Physics*, vol. 51, no. 4, pp. 410–413, 2005.

[14] S. E. Schmidt, H. Zimmermann, J. Hansen and H. Møller, "The chest is a significant collector of ambient noise in heart sound recordings," in *Computing in Cardiology*, Krakow, 2012 .

[15] P. Hasgall, "IT'IS Database for thermal and electromagnetic parameters of biological tissues," Version 4.0, DOI: 10.13099/VIP21000-04-0. https://itis.swiss/virtual-population/tissue-properties/database/acoustic-properties/speed-of-sound/, 2018.

[16] "University of Notre Dame – Physics in medicine," [Online]. Available: https://www3.nd.edu/~nsl/Lectures/mphysics/index.htm. [Accessed October 2019].

[17] S. Mohammadi, . A. Hedjazi, M. Sajjadian and N. Ghoroubi, "Study of the normal heart size in Northwest part of Iranian population: A cadaveric study," *Cardiovascular and Thoracic Research*, vol. 8, no. 3, pp. 119–125, 2016.

[18] "Auscultatory Sites," [Online]. Available: http://www.stethographics.com/heart/main/sites.htm. [Accessed 2019].

[19] S. Leng, R. S. Tan and K. C. T. Chai, "The electronic stethoscope," *BioMedical Engineering OnLine*, vol. 14, no. 66, 2015.

[20] L. Nowak and N. Nowak, "Sound differences between electronic and acoustic stethoscopes," *BioMedical Engineering OnLine*, vol. 17, no. 1, 2018.

[21] S. Sato, T. Koyama, K. Ono, G. Igarashi, H. Watanabe and H. Ito, "Cardiac diagnosing by a piezoelectric-transducer-based heart sound monitor system," in *Proceedings of the International Conference on Biomedical Electronics and Devices*, Rome, Italy, 2011.

[22] G. Nelson and R. Rajamani, "Improved auscultation with a stethoscope using model inversion for unknown input estimation," in *American Control Conference (ACC)*, Boston, MA, pp. 3970–3975, 2016.

[23] M. B. Hawes and W. Liu, "Sparse microphone array design for wideband beamforming," in *18th International Conference on Digital Signal Processing (DSP)*, Fira, 2013.

[24] J. Benesty, J. Chen and Y. Huang, *Microphone array signal processing*, Verlag Berlin Heidelberg: Springer, 2008.

[25] W. Ser, H. Chen and Z. L. Yu, "Self-calibration-based robust near-field adaptive beamforming for microphone arrays," *Transactions on Circuits and Systems II: Express Briefs*, vol. 54, no. 3, pp. 267–271, March 2007.